732 (1965); R. Weber and P. E. Tannenwald, Phys. Rev. 140, A498 (1965).

[8]C. Kittel, Phys. Rev. 110, 1295 (1958); P. Pincus, *ibid.* 118, 658 (1960); J. W. Hartwell, Proc. IEEE 56, 23 (1968).

[9]The angular dependence of ferromagnetic resonance has also been examined. C. Vittoria, R. C. Barker, and A. Yelon, J. Appl. Phys. 40, 1561 (1969). See also Ref. 10.

[10]R. F. Soohoo, J. Appl. Phys. Suppl. 32, 148S (1961).

[11]G. I. Lykken, Phys. Rev. Letters 19, 1431 (1967).

[12]M. Sparks, B. R. Tittmann, J. E. Mee, and C. Newkirk, J. Appl. Phys. 40, 1518 (1969).

[13]R. E. De Wames and T. Wolfram, J. Appl. Phys. 41, 987 (1970).

[14]T. G. Phillips, L. W. Rupp, Jr., A. Yelon, R. C. Barker, and C. Vittoria, J. Phys. (Paris) 32, C1-1162 (1971).

[15]O. Horan, G. C. Alexandrakis, and C. N. Manicopoulos, Phys. Rev. Letters 25, 246 (1970); B. Heinrich and V. F. Meshcheryakov, Zh. Eksperim. i Teor. Fiz. Pis'ma v Redaktsiyu 9, 618 (1969) [Sov. Phys. JETP Letters 9, 378 (1969)].

[16]See, for example, A. I. Akhiezer, V. G. Bar'yakhar, and S. V. Pepetimnski, *Spin Waves* (North-Holland, Amsterdam, 1969).

[17]The matrix treatment of the boundary conditions was suggested by R. L. Walker (private communication).

[18]R. E. DeWames and T. Wolfram, Phys. Rev. Letters 26, 1445 (1971); T. Wolfram and R. E. De Wames, Solid State Commun. 9, 171 (1971).

[19]See, for example, P. M. Morse and H. Feshback, *Methods of Theoretical Physics* (McGraw-Hill, New York, 1953), Vol. 1, p. 215.

[20]R. Weber, P. E. Tannenwald, and C. H. Bajorek, Appl. Phys. Letters 16, 35 (1970).

PHYSICAL REVIEW B VOLUME 4, NUMBER 9 1 NOVEMBER 1971

Two-Exciton Transitions in MnF_2 and $RbMnF_3$

S. E. Stokowski, D. D. Sell, and H. J. Guggenheim
Bell Telephone Laboratories, Murray Hill, New Jersey 07974

(Received 9 June 1971)

Absorption lines corresponding to the simultaneous creation of two excitons have been investigated in MnF_2 and $RbMnF_3$. The particular zero-phonon transitions observed are those from the ground states of a Mn ion pair to the $^4T_1(G)+{}^4T_1(G)$, $^4T_1(G)+{}^4A_1$, ^4E, and $^4T_1(G)+{}^4T_2(D)$ excited states in MnF_2 and to the $^4T_1(G)+{}^4T_1(G)$, $^4T_1(G)+{}^4A_1$, ^4E, and $^4A_1$, $^4E+{}^4A_1$, ^4E states in $RbMnF_3$. An attempt is made to identify the particular excitons created in these transitions through their polarizations and uniaxial stress behavior. Selection rules are derived using the space-group representations along with the additional assumption that the transition mechanism is an off-diagonal exchange interaction between pairs of Mn ions on opposite magnetic sublattices. The interaction between excitons is discussed; it is found experimentally that for those excitons which couple strongly to the lattice, the phonon coupling provides the major part of the interaction. The exciton-exciton interaction energy is positive or negative and varies from 10 to 400 cm^{-1} in magnitude. A measurement of the L-point magnon energy in $RbMnF_3$ has been made from an analysis of the $^6A_1 \rightarrow {}^4T_1(G)$ magnon sidebands; it is found to be 73 ± 0.5 cm^{-1}.

I. INTRODUCTION

The creation of more than one quasiparticle upon the absorption of a photon is a general feature in the spectra of many solids and occurs whenever there is an interaction between the quasiparticles. The quasiparticles about which we are speaking could be, for example, phonons, excitons, or magnons. By definition, photon absorption involving the creation of several quasiparticles is weak, since presumably the particle states have been constructed so that the two-particle interactions are small. However, if the one-particle transition is forbidden in some way, the pair or multiple transitions can be a relatively important feature in the absorption spectrum. Two-particle or pair transitions have been observed in the spectra of antiferromagnetic insulators, α-O_2,[1] and possibly silicon.[2] Pair transitions have also been seen for pairs of impurity ions in solids.[3-5]

The pair transitions in antiferromagnetic insulators have been studied in considerable detail. These transitions include combinations of two important quasiparticles present in magnetic systems: magnons and excitons. The absorption spectra of these substances exhibit exciton-magnon,[6,7] two-magnon,[8] and two-exciton transitions.[9] These processes have been of interest because of their intimate relationship with the exchange interaction between ions. Further, they have been useful in studying the properties of excitons and magnons. In this paper we shall concern ourselves with the two-exciton transitions in MnF_2 and $RbMnF_3$.

This work was motivated by our earlier work[10] on two-exciton lines in MnF_2, in which the lowest two-exciton states were observed and identified. In order to understand the source of the interaction between excitons and the strengths of the two-ex-

citon lines and also to investigate exciton dispersion and intersublattice exchange of excitons, we decided to look at a number of exciton-exciton transitions in different crystals. The crystals MnF_2 and $RbMnF_3$ were chosen: MnF_2 because of the large body of knowledge about its properties, and $RbMnF_3$ because its high symmetry and different crystal structure provide a good comparison with MnF_2.

Several two-exciton absorption lines were observed in both materials and are reported in Sec. IV. In the same section we present the uniaxial stress behavior of some of the absorption lines, which was used for identification purposes. Selection rules for the two-exciton transitions and possible sources of the exciton-exciton interaction are discussed in Sec. II. Experimentally it is found that this interaction arises primarily from exciton-phonon coupling for those excitons which couple strongly to the lattice and can be either attractive or repulsive.

II. THEORY

MnF_2 has the rutile structure with the paramagnetic space group $P4_2/mnm$ (D_{4h}^{14}). Below the Néel temperature the magnetization lies along the c axis, and the optically active Mn^{2+} ion has a unitary site symmetry C_{2h}. The Mn^{2+} ion has two Mn nearest neighbors (NN) on the same magnetic sublattice, 3.31 Å away along the c axis, and eight second NN on the opposite magnetic sublattice, 3.78 Å away. The bond angle for a first NN pair is 102°, with a ground-state exchange constant $J_1 = 0.22$ cm^{-1}; whereas, a second NN pair has a 129° bond angle and an exchange constant $J_2 = -1.22$ cm^{-1}.[11-13]

$RbMnF_3$ has the perovskite structure with a paramagnetic space group $Pm3m$ (O_h^1). Below the Néel temperature the unitary site symmetry of the Mn^{2+} ion is C_{4h} if the magnetization ($\vec{M}$) lies along a [001] cubic axis and C_{3i} if $\vec{M}$ is parallel to $\langle 111\rangle$. The anisotropy field is very small (~4 Oe) with the equilibrium direction being $\langle 111\rangle$[14]; therefore, it is relatively easy to reorient the magnetization with an applied stress or magnetic field. The Mn^{2+} ion has six Mn first NN, 4.26 Å away on the opposite magnetic sublattice, and twelve second NN, 6.02 Å away on the same sublattice. $RbMnF_3$ has a 180° exchange between the first NN Mn pairs, with $J_1 = 2.35$ cm^{-1}.[15] The exchange constant J_2 is 0.00 ± 0.2 cm^{-1}. The smallness of J_2 is not surprising, because there is no direct path for the superexchange interaction in this case.

In both crystals the Mn^{2+} ion is surrounded by an octahedron of fluorine ions, but in MnF_2 this is distorted to orthorhombic symmetry. The energy levels of Mn^{2+} in both crystals have the same ordering, but they are somewhat lower in $RbMnF_3$ by ~200 cm^{-1}. The ionic states of primary interest to us here are the $^6A_1$ ground state ($t_2^3 e^2$ configuration), the lowest excited state, $^4T_1$ (96% $t_2^4 e$ configuration), and the $^4A_1, ^4E$ (G) states ($t_2^3 e^2$ configuration). We shall first derive the selection rules for the two-exciton transitions and then discuss the exciton-exciton interaction.

A. Selection Rules

Two-exciton absorption consists of the creation of two excitons with wave vectors $\vec{k}$ and $-\vec{k}$ with one photon ($\vec{k} \sim 0$). It is a straightforward problem[16] to determine the selection rules once the group representations of the excitons are known. These rules provide us with information on the polarization of transitions for the creation of two excitons with wave vectors throughout the Brillouin zone. However, this approach is useful only if the energy dispersion of the excitons separate out the various critical points. On the other hand, if the dispersion of the excitons is smaller than the experimental energy resolution, then all points in the Brillouin zone can contribute to an observed transition, and the space-group selection-rule information is averaged out. Fortunately, we can assume that the interactions between the magnetic ions have a higher symmetry than that of the crystal. An example of such an interaction is the Heisenberg isotropic exchange. For the two-magnon, exciton-magnon, and two-exciton transitions the assumption is made that the interaction giving rise to these excitations occurs between pairs of electrons or, equivalently, pairs of ions and has the form

$$\sum_{i,j} (\vec{E}\cdot\vec{\pi}_{ij})(\vec{s}_i\cdot\vec{s}_j) , \tag{1}$$

where i and j refer to electrons on the spin-down and spin-up sublattices, respectively, $\vec{\pi}_{ij}$ is a transition dipole moment, and $\vec{s}_i$, $\vec{s}_j$ are generalized spin operators which can operate on the orbital and spin states of the electrons. Such an interaction, which involves off-diagonal exchange terms, was first introduced by Tanabe, Moriya, and Sugano,[17] and actual expressions for the π_{ij}'s were obtained by Gondaira and Tanabe.[18]

Upon summing over the electrons on both ions, a pair transition moment $\vec{P}_{ab}(e_a e_b)$ will be obtained for the two-exciton transition, where the ion a is excited from the ground state g_a to an excited state e_a, and equivalently for the ion b. In order that a given component of $\vec{P}_{ab}$ be nonzero, the product representation $(e_a \times g_a) \times (e_b \times g_b)$ must transform as that component for those operations which leave the pair invariant. The determination of the nonzero pair transition moments provides us with more information than the space-group selection rules for a $(\vec{k}, -\vec{k})$ exciton pair, since we are assuming a specific interaction between the excitons. To include the full space-group symmetry of the system, one sums the pair moments of the equivalent pairs,

TABLE I. Electric dipole selection rules for the two-exciton transitions at the critical points in MnF_2. The parentheses indicate that the transition is not allowed if the two excitons are identical.

	Z	A	X
Γ_1^+, $\Gamma_2^+ + \Gamma_1^+$, Γ_2^+	(π)	π	σ
Γ_3^+, $\Gamma_4^+ + \Gamma_3^+$, Γ_4^+	(π)	π	σ
Γ_1^+, $\Gamma_2^+ + \Gamma_3^+$, Γ_4^+	σ	σ	π

$E1$ and $E2$ both transform as Γ_1^+, Γ_2^+
$^4T_1(0, \pm\frac{3}{2})$ transform as Γ_3^+, Γ_4^+
$(^4E\theta, \pm\frac{3}{2})$ and $(^4A_1 \pm\frac{3}{2})$ transform as Γ_3^+, Γ_4^+
$(^4E\epsilon, \pm\frac{3}{2})$ transform as Γ_1^+, Γ_2^+

each one being multiplied by the appropriate phase factor for the given wave vector $\vec{k}$ of the excitons. This approach was used previously in explaining the polarization properties of the $^4T_1 + {}^4T_1$ absorption lines in MnF_2.[10] (In this paper excitons will commonly be labeled by the final excited state, since the initial state is always the $^6A_1$ ground state, e.g., "$^4T_1$ exciton" in place of "$^6A_1 \rightarrow {}^4T_1$ exciton." The two-exciton transitions are indicated by a plus sign between the two excitons.)

We first consider here the selection rules for MnF_2. The $k = 0$ excitons transform either as Γ_1^+, Γ_2^+ or as Γ_3^+, Γ_4^+ of the factor group D_{2h}.[19] The selection rules for the two-exciton transitions are given in Table I. These rules have some usefulness in the case of the $^4T_1 + {}^4A_1, {}^4E$ transitions where the $^4E\theta$ exciton has a -74-cm^{-1} dispersion along Z.[19] Next, for a determination of the nonzero pair transition moments we use the symmetry of a second NN Mn pair, C_s', a time-reversal mirror plane containing the c axis and the pair axis. The pair moments for the $^4T_1 + {}^4T_1$ transitions were determined in a previous paper.[10] In the case of the $^4T_1 + {}^4A_1, {}^4E$ transitions, it is found that the pair symmetry allows both σ and π polarizations for the two-exciton lines.

The symmetries for a first nearest-neighbor Mn pair in $RbMnF_3$ are given in Table II for different orientations of the spins. The equilibrium spin directions in unperturbed $RbMnF_3$ are the $\langle 111 \rangle$ axes. For unstressed $RbMnF_3$ no polarization of any absorption lines was seen, which indicates the presence of domain averaging and agrees with previous observations of domains by antiferromagnetic resonance techniques.[20] Upon applying a [001] uniaxial stress greater than 420 bars, a single domain is formed with the sublattice magnetizations along [001].[21] In this situation one would expect to see polarized two-exciton lines, and thus, we derive the selection rules for a [001] spin orientation.

We shall proceed directly to a calculation of the rules for the transition moments, since the space-group selection rules do not provide useful information. The representations of the single-ion transitions on the two sublattices are indicated in Fig. 1 for the [001] spin orientation (ion-site group C_{4h}). Since the pair has inversion combined with time-reversal symmetry, a very important parity–time-reversal selection rule results, The rule is that the pair transition is forbidden if the final electronic states on the two ions are a time-reversed pair, that is, identical except for time reversal.

For an ion pair, the unitary operations which leave the pair invariant and do not interchange the ions form the group C_4 for the [001]-oriented pair and C_s for the [100]- and [010]-oriented pairs. Thus, the C_{4h} exciton representations are reduced to these groups for the pair excitation. The representations of the two-exciton state in the above groups are simply the direct product of the exciton representations on the two sublattices, which leads to selection rules given in Table III. The parity–time-reversal symmetry is used implicitly in the construction of this table.

B. Exciton-Exciton Interactions

The exciton-exciton interaction energy is defined as the difference between the energy of the two-exciton state and the sum of the one-exciton energies. There are two important contributions to this interaction: lattice coupling and excited-state exchange.

First, consider the interaction via lattice coupling. Since an exciton is accompanied by a lattice displacement, the size of which depends on the exciton-phonon coupling, two neighboring excitons can interact through these lattice distortions. The

TABLE II. Symmetry groups for a first nearest-neighbor Mn pair with different spin orientations in $RbMnF_3$. The unitary factor groups are indicated by the parentheses. The group which both leaves the pair invariant and does not interchange the Mn ions is given in the column labeled ion-site symmetry.

Spin direction	Pair symmetry	Ion-site symmetry
[001]	$D_{4h}'(D_4)$	$C_{4v}'(C_4)$
[010], [100]	$D_{2h}'(D_2)$	$C_{2v}'(C_s)$
$\langle 111 \rangle$	$C_{2h}'(C_2)$	$C_s'(C_1)$

TABLE III. Selection rules for two-exciton transitions in $RbMnF_3$ for the magnetization along [001].

Pair axis	Ion-site group	Exciton product representations	Polarization
[001]	C_4	$(\Gamma_1^+$ or $\Gamma_2^+) \times (\Gamma_3^+$ or $\Gamma_4^+)$	$\vec{E} \perp [001]$
		$(\Gamma_3^+ \times \Gamma_3^+)$ or $(\Gamma_4^+ \times \Gamma_4^+)$	...
		$\Gamma_1^+ \times \Gamma_2^+$	...
[100] or [010]	C_s	$(\Gamma_1^+$ or $\Gamma_2^+) \times (\Gamma_3^+$ or $\Gamma_4^+)$	$\vec{E} \parallel [001]$
		$(\Gamma_3^+ \times \Gamma_3^+)$ or $(\Gamma_4^+ \times \Gamma_4^+)$	$\vec{E} \perp [001]$
		$\Gamma_1^+ \times \Gamma_2^+$	$\vec{E} \perp [001]$

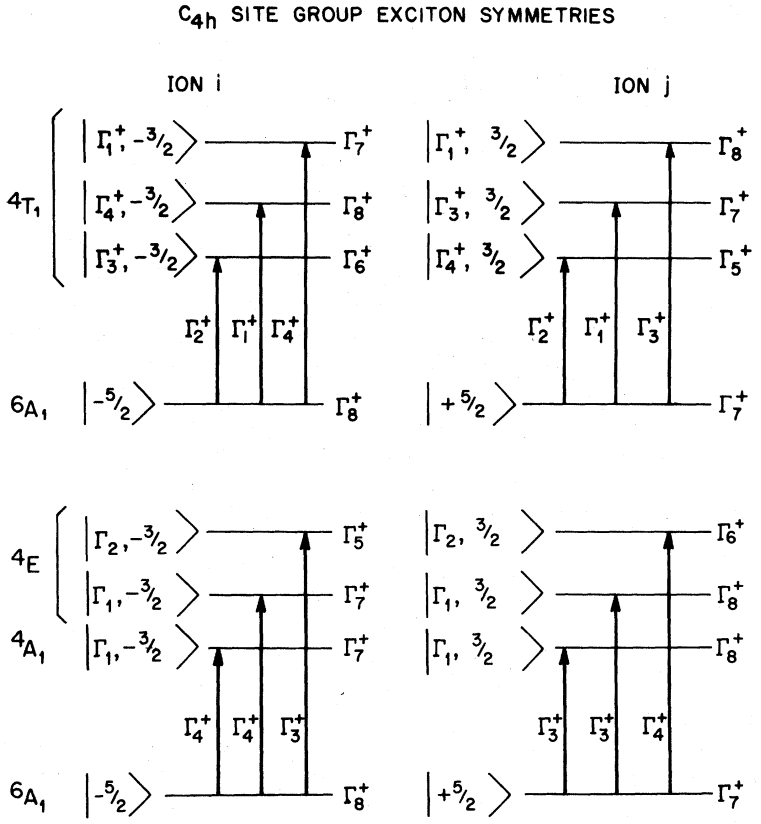

FIG. 1. Group representations of sublattice excitons for C_{4h} site symmetry. The two ions are on opposite magnetic sublattices.

amount of exciton-lattice coupling can be determined from experiment by comparing the strength of the phonon band to the zero-phonon line strength, the ratio of which is commonly indicated by e^{-S}, where S is the Huang-Rhys factor. In MnF_2 and $RbMnF_3$ we must obtain this factor by comparing the intensity of the exciton-magnon band to that of the phonon band, which is in actuality an exciton-magnon-phonon band. The $^4T_1(G)$ exciton-magnon band has a Huang-Rhys factor (S) of ~4.5 in both materials, indicating a sizeable lattice distortion; whereas the $^4A_1$, $^4E(G)$ and the $^4T_2(D)$ exciton-magnon transitions do not show much phonon cooperation. Thus, this contribution to the interaction between excitons will be larger for those processes creating $^4T_1$ excitons than for those in which $^4A_1$, ^4E excitons are created.

The other important contributor to the two-exciton interaction is the dependence of exchange energy on the electronic state of the ions. The exchange between the electrons of an Mn^{2+} pair can be written

$$H_{ex}=\sum_{i,j} J_{aibj}\,\vec{S}_{ai}\cdot\vec{S}_{bj}\ , \qquad (2)$$

where a and b refer to the two ions of the pair. [The exchange parameters J_{aibj} may depend on the spin states of the ions, in which case a term of the form $J_{ijkl}(\vec{S}_i\cdot\vec{S}_j)(\vec{S}_k\cdot\vec{S}_l)$ could be added to expression (2).]

The exchange energy for an Mn pair in the ground state can be written $J_0\vec{S}_a\cdot\vec{S}_b$, where

$$J_0=\frac{1}{S_aS_b}\sum_{i,j} J_{aibj}\ .$$

The exchange field that an Mn^{2+} ion sees is $J_0Sz/g\beta$, where z is the number of nearest neighbors. If one ion is in an excited state, we have

$$H_{ex}=J'\vec{S}'_a\cdot\vec{S}_b\ , \qquad (3)$$

where J' is a new linear combination of the J_{aibj}'s, the combination depending on the particular excited state. The exchange field experienced by a Mn^{2+} ion in an excited state is then $J'Sz/g\beta$. If two neighboring ions are excited, the exchange field becomes $[J''S'+(z-1)J'S]/g\beta$, where $J''S'_a\cdot S'_b$ is the exchange between the two excited Mn ions. Thus, the exchange contribution to the exciton-exciton interaction energy is

$$\Delta=2S'[SJ'-S'J'']\ . \qquad (4)$$

The relative importance of these two contributions to the exciton-exciton interaction is difficult to estimate theoretically. However, the exchange contribution would appear to be on the order of a pair exchange energy or less (~20 – 25 cm^{-1} for MnF_2 and $RbMnF_3$). Experimentally we find that the $^4T_1+{}^4T_1$ transitions in $RbMnF_3$ show a 400-cm^{-1}

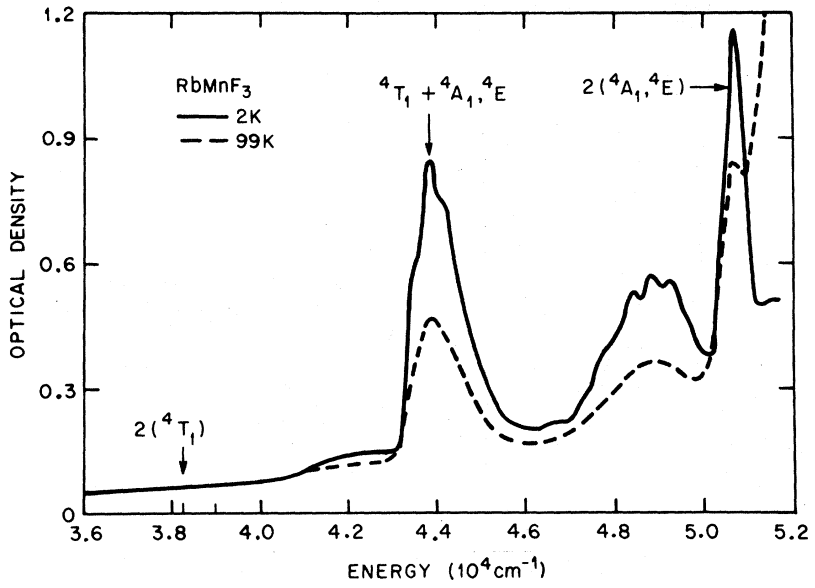

FIG. 2. Transmission spectrum of a 0.1-mm-thick sample of $RbMnF_3$ at $T = 2$ and 99 K.

exciton-exciton interaction energy. This energy is larger than one would expect from the exchange contribution alone, and therefore implies that the phonon contribution is dominant in this case. On the other side, the $^4T_1(G) + {}^4T_2(D)$ transitions in MnF_2 and the double $^4A_1$, ^4E lines in $RbMnF_3$ have interaction energies less than 10 cm^{-1}. This could arise either from weak phonon coupling or exchange interactions.

III. EXPERIMENTAL DETAILS

Our absorption measurements were made with a double-beam spectrophotometer described in a previous paper.[22] A 75-W Xe arc was used as the light source. Since most of the light from a Xe arc is in the visible range, the visible light must be removed before it reaches the entrance slit of the spectrometer. Otherwise, unwanted visible light passes through the exit slit because of scattering within the instrument. A quartz wedge plate was used to predisperse the source light before it reached the entrance slit. With this arrangement the amount of scattered visible light incident on our detector was less than 1% of the uv light, even at 2000 Å. The smallest change in transmission detectable with our apparatus was 5 parts in 10^3 at 2000 Å with 0.8-Å resolution, and 4 parts in 10^3 at 2200 Å with 0.2-Å resolution. The uniaxial stress measurements were made on $1\times5\times5$-mm or $1\times3\times5$-mm samples; the stress was applied to the samples via a pneumatic apparatus described in an earlier paper.[23] The MnF_2 and $RbMnF_3$ samples were grown with zone-refined MnF_2 and RbF material using a modified Bridgman technique. The narrow linewidths that we observed for the exciton transitions indicated the material was of good quality.

IV. RESULTS

Figures 2 and 3 show the absorption spectra of $RbMnF_3$ and MnF_2, respectively. These curves are similar to those obtained by Ferguson[9] on both substances and by Mehra and Venkateswarlu[24] on $RbMnF_3$, except that we have observed additional band and sharp-line structure due to the lower temperature and higher resolution in our measurements. We have also extended the measurements up to an energy of 51 000 cm^{-1} and have seen the $^4A_1, {}^4E + {}^4A_1, {}^4E$ two-exciton band in $RbMnF_3$ for the first time. The same band was not seen in MnF_2 because a 0.1-mm-thick sample of MnF_2 is essentially opaque (transmission < 1%) above 49 000 cm^{-1}, indicating an absorption coefficient greater than 500 cm^{-1}. It is not known whether this strong absorption comes from the two-exciton bands in this region or from the onset of transitions from bonding to antibonding states. It does seem likely, in view of the apparent sizable oscillator strength, that it is the latter case.

For comparison, the absorption spectra taken at $T = 99$ K are also shown in Figs. 2 and 3. It can be seen that the oscillator strengths of the two-exciton bands at 2 K are approximately a factor of 2 larger than those at 99 K. In contrast, the $^4A_2$ one-exciton band at ~40 000 cm^{-1} in both MnF_2 and $RbMnF_3$ does not have this increase. According to a calculation by Druzhinin *et al.*,[25] the temperature dependence of the two-exciton strength is related to the spin correlation between the two magnetic sublattices. This temperature behavior of the oscillator strengths is useful in distinguishing the two-exciton transitions. Table IV lists the various

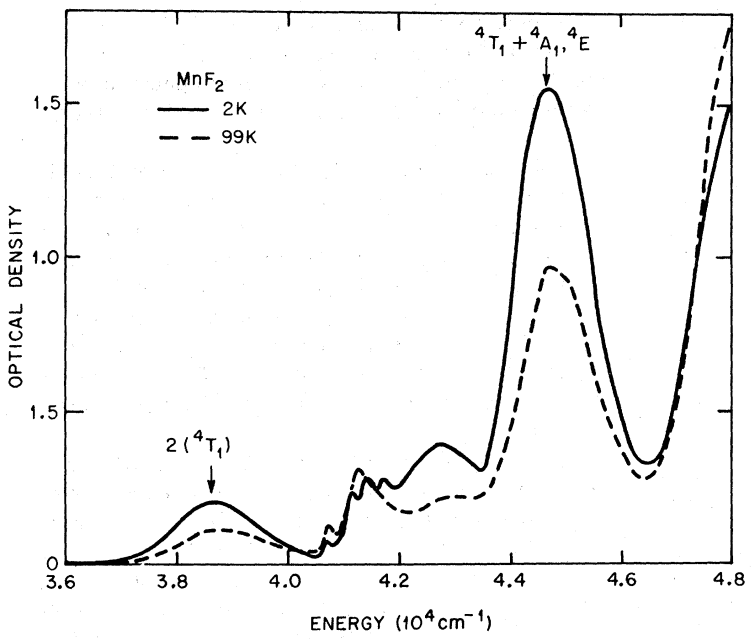

FIG. 3. Transmission spectrum of a 1-mm-thick sample of MnF_2 at $T = 2$ and 99 K.

possible two-exciton bands along with their expected and observed positions. We now proceed to a description and discussion of the observed two-exciton lines, considering each state in turn.

A. MnF_2

The one-exciton and exciton-magnon absorptions in MnF_2 have been studied by Sell *et al.*[7] and by Meltzer and Lohr.[26] Uniaxial stress measurements on the exciton and exciton-magnon transitions have been performed by Dietz *et al.*[27] on the $^4T_1$ excitons and by Meltzer *et al.*[19] on the $^4A_1$, ^4E excitons. The details of the one-exciton spectra are reasonably well understood. The two lowest-energy excitons, at 18 419 ($E1$) and 18 436 cm^{-1} ($E2$), are constructed from linear combinations of the $(\pm 1, -\frac{3}{2})$ substates of the $^4T_1$ manifold.[22] The observed excitons of the $^4A_1$ and ^4E states are the $^4E\epsilon$ exciton at 25 245 cm^{-1} and the $^4E\theta$ exciton at 25 260 cm^{-1}. Meltzer *et al.* found that the $^4E\theta$ exciton has a -74-cm^{-1} dispersion from Γ to Z in the Brillouin zone, but very little dispersion along the x direction.

1. $^4T_1(G) + {}^4T_1(G)$

Most of the work on this state was reported in a previous paper[7]; however, one interesting result was not discussed. These data provide an upper bound for the frequency of the intersublattice exchange of the $E1$ and $E2$ excitons. It was found that the transitions $E1(A) + E2(B)$ and $E2(A) + E1(B)$, labeled E_{12} and E_{21}, respectively, are degenerate; A and B refer to the two sublattices. This degeneracy can be split by a [110] stress, which makes the two sublattices inequivalent. These two-exciton states are not required to be degenerate, since the two excitons could interchange sublattices. In other words, there can be an interaction between E_{12} and E_{21} such that the eigenstates become $2^{-1/2}(\psi_{12} \pm \psi_{21})$ with energies $\pm\langle\psi_{12}|H_{\rm int}|\psi_{21}\rangle$, a type of Davydov splitting. The single exciton Davydov splitting arising from an intersublattice transfer of one exciton is small experimentally because it involves a $\Delta M_s = 2$ process. However, since the intersublattice crossing of two excitons is a $\Delta M_s = 0$ process, it might have a larger probability.

We observed that E_{12} and E_{21} are degenerate to within 4 cm^{-1}; therefore, the matrix element $\langle\psi_{12}|H_{\rm int}|\psi_{21}\rangle$ is less than 2 cm^{-1} and thus an upper limit on the intersublattice crossing frequency of two excitons is 6×10^{10} sec^{-1}. An estimate of the interaction matrix, which is an off-diagonal Coulomb term, can be obtained from a calculation of Fuchikami on $KMnF_3$.[28] She obtains a value of 2–4 cm^{-1} for these particular Coulomb integrals.

TABLE IV. Two-exciton band energies.

Final states	Band energies ($10^3 cm^{-1}$)			
	MnF_2		$RbMnF_3$	
	Expected	Observed	Expected	Observed
$^4T_1(G) + {}^4T_1(G)$	38.8	38.7	38.3	38.3
$^4T_1(G) + {}^4T_2(G)$	43.0	42.9	42.3	42.2
$^4T_1(G) + {}^4A_1, {}^4E(G)$	44.9	44.7	44.6	43.9, 44.2
$^4T_2(G) + {}^4T_2(G)$	47.2	47.1	46.2	(46.7)
$^4T_1(G) + {}^4T_2(D)$	47.9		47.4	47.3 (47.8)
$^4T_2(G) + {}^4A_1, {}^4E(G)$	49.1		48.5	48.4 (48.9)
$^4T_1(G) + {}^4E(D)$	49.7		49.4	49.2
$^4A, {}^4E + {}^4A, {}^4E$	51.0		50.8	50.8
$^4T_2(G) + {}^4T_2(D)$	52.1		51.3	
$^4T_1(G) + {}^4T_1(P)$	52.2		51.9	

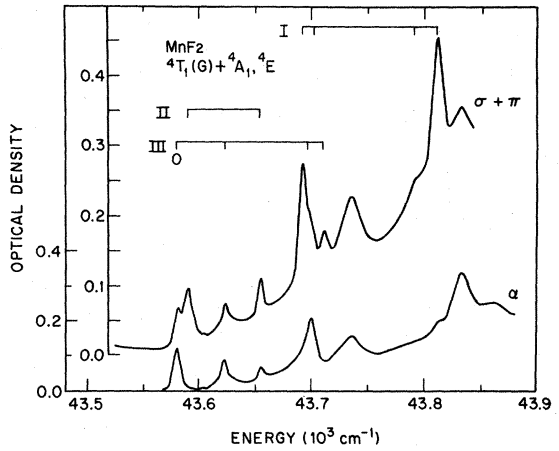

FIG. 4. Absorption spectrum in the $^4T_1(G)+{}^4A_1$, ^4E two-exciton region for a 1-mm-thick MnF_2 crystal. The ordinate zero is arbitrary. Note that the optical density scale for the α spectrum is a factor 2 smaller than that for the $\sigma+\pi$ curve in order that a direct comparison of the intensities of the two spectra can be made. The three groups of lines labeled I, II, and III are discussed in the text.

Although the above calculation is for $KMnF_3$, we might expect the order of magnitude to be correct for MnF_2. If the lattice distortions associated with E_{12} and E_{21} are different, the interaction matrix is reduced by $S(0,0)<1$, the amount of vibronic overlap between the two double-exciton states. Thus, the fact that no splitting is observed is consistent with these theoretical estimates.

2. $^4T_1(G)+{}^4A_1$, ^4E

This should be one of the more interesting two-exciton combinations to study because of the -74-cm^{-1} dispersion of the $^4E\theta$ exciton. Figure 4 shows the $\alpha(\vec{k}\parallel c)$ (lower curve) and the $\vec{k}\perp c$ spectra (upper curve). The $\vec{k}\perp c$ spectrum contains about equal amounts of σ- and π-polarized light. Table V lists the energies of what appear to be zero-phonon lines and their polarizations. The excitons from the $^4T_1$ manifold which may contribute in this region are the lowest two excitons ($E1$ and $E2$) and possibly the exciton from the $^4T_1(0,\pm\frac{3}{2})$ state, which is not observed in the one-exciton spectrum but is calculated to be about 50–60 cm^{-1} above the $E1$ energy by Meltzer and Lohr.[26] The dispersion energy of the $^4T_1$ excitons is less than 0.5 cm^{-1}.[29] From the ^4A,^4E manifold we have the three orbital states $^4A_1$, $^4E\theta$, and $^4E\epsilon$. The $^4E\epsilon$ excitons have been observed in the one-exciton spectrum, but the energy of the $^4A_1$ exciton has not been definitely established. The $^4E\theta$ exciton has been shown to have a -74-cm^{-1} dispersion in the z direction and little dispersion along x. Therefore, the energy of the $^4E\theta$ exciton at the X point is 74 cm^{-1} higher than it is at the Z and A points in the Brillouin zone. It is also observed that the dispersion of the $^4E\epsilon$ exciton is small.[19] Therefore, in the $^4A_1$, $^4E+{}^4T_1(G)$ two-exciton spectrum we would expect at least six lines, possibly fifteen lines.

The selection rules for the two-exciton transitions at total $\vec{k}=0$ are given in Table I. Note that if any dispersion of the $E\theta$ or A_1 excitons is to be seen, it will appear in the σ spectrum. We are now left with the problem of identification. Since the stress behavior of the two-exciton states was useful in the identification of the $^4T_1+{}^4T_1$ exciton spectrum, we studied these $^4A_1$, $^4E+{}^4T_1$ excitons for various levels of [001] uniaxial stress up to 1.5 kbars.

The following results were obtained: (i) The four lines at 112, 119.5, 211, and 231 cm^{-1} away from the first line at 43 580 cm^{-1} shift downward in energy as the $E1$ exciton (12 cm^{-1}/kbar). These lines are labeled group I in both Fig. 4 and Table V. (The $E1$ exciton is the only one with a sizable energy shift under [001] stress. The stress dependences of the other exciton energies are small, being -1.2, $+2$, and $+0.6$ cm^{-1}/kbar for the $E2$, $^4E\epsilon$, and $^4E\theta$ excitons, respectively.) (ii) The two lines at 9 and 74 cm^{-1} shift upwards slightly (~ 3 cm^{-1}/kbar). These are labeled group II. (iii) The three lines at 0, 42, and 131 cm^{-1} appear to move less than 2 cm^{-1}/kbar. These are labeled group III. (iv) An additional line, not resolved at zero stress, appears at 117 cm^{-1} and probably has the stress behavior of the group-III lines.

The 231-cm^{-1} peak in group I is very likely a phonon sideband of the 122-cm^{-1} line, since harmonics of it appear in the phonon band out to at least the 10th overtone. The 211-cm^{-1} peak may also be a phonon-assisted transition. Therefore, we are inclined to assign the two lines at 112 and 119.5 cm^{-1} to the $E1+{}^4E\theta$ and $E1+{}^4E\epsilon$ transitions. The sum of the individual $E1$ and $E\theta$ ($E\epsilon$) exciton energies is 43 665 cm^{-1} (43 680 cm^{-1}), which falls below the observed two-exciton energy by about 25 cm^{-1}. Since no line below these has an $E1$

TABLE V. Two-exciton line energies.

Two-exciton state	Energies (cm^{-1})
MnF_2: $^4T_1(G)+{}^4A_1$, ^4E	Origin at 43 580
	I 112(π), 119.5(σ), 211(π), 231(π,σ)
	II 9(π), 74(π,σ)
	III 0.0(σ), 42(σ), 131(π), 23(σ)
$^4T_1(G)+{}^4T_2(D)$	46 377; 46 393; 46 413; 46 417
$RbMnF_3$: $^4T_1(G)+{}^4T_1(G)$	Origin at 36 832
	-5, 0.0, 47, 51, 85, 92, 152
$^4T_1(G)+{}^4A$, $^4E(G)$	Origin at 43 302
	0.0, 5, 58, 91, 96
$^4A_1, {}^4E(G)+{}^4A_1, {}^4E(G)$	50 281; 50 351;(?); 50 366(?)

stress behavior, except perhaps for the weak 23-cm^{-1} line, whose stress behavior we cannot observe, it appears that we are not seeing transitions in which the $E1+E\theta$ excitons are created at the Z,A points. If the 23-cm^{-1} line is $E1+E\theta$ at Z and A, then this would imply a negative dispersion of 89 cm^{-1}. (We could expect that the -74-cm^{-1} dispersion of the $E\theta$ exciton would be modified by the exciton-exciton interaction.)

Any further assignments in this region are at the moment to be considered as rather tentative. However we suggest that the 117- and 131-cm^{-1} lines are the $E2+E\epsilon$ and $E2+E\theta$ transitions and the 42-cm^{-1} line is $E2+E\theta$ at the Z,A point. The π-polarized lines at 9 and 74 cm^{-1} which shift upward by 3 cm^{-1}/kbar under [001] stress, do not have a stress behavior consistent with any combination of $E1$, $E2$ and $E\epsilon$, $E\theta$ excitons and, therefore, possibly are associated with either the ^4A or other $^4T_1$ excitons.

3. $^4T_1(G)+{}^4T_2(D)$

Four sharp lines are observed close to the expected positions of the $^4T_1(G)+{}^4T_2(D)$ two-exciton states. (Their energies are listed in Table V.) These have peak absorption coefficients of about 3 cm^{-1} and linewidths of 5 cm^{-1}, with the first line being only about $\frac{1}{9}$ the intensity of the others. Only one exciton at 27 983 cm^{-1} is seen for the $^6A_1 \rightarrow {}^4T_2(D)$ transitions. It appears in π-polarized light and thus is a Γ_3, Γ_4 exciton. No attempt has been made to identify the two-exciton lines.

B. $RbMnF_3$

The $^4T_1$ and $^4A_1$, ^4E single excitons and exciton-magnon transitions in $RbMnF_3$ have been studied by Chen *et al.*[30] They observed two of the $^4T_1$ excitons at 18 221 and 18 227 cm^{-1}. We find these excitons at energies of 18 229 and 18 234 cm^{-1}.[31] A third transition at 18 239 cm^{-1} is observed when a [001] uniaxial stress is applied to the sample. Our results indicate that it apparently has a very small intensity (absorption coefficient $< 6\times10^{-3}$ cm^{-1}) in the unstressed crystal. Chen *et al.* have assigned these three lowest excitons to those constructed from the $l_z=\pm1, 0$, $m_s=\frac{3}{2}$ substates of the $^4T_1$ manifold, the 5-cm^{-1} splitting being due to the spin-orbit interaction. From this 5-cm^{-1} splitting they extracted a value of 19 cm^{-1} for the spin-orbit parameter ζ_{3d} instead of its usual value of 300 cm^{-1}, and suggested that it was quenched by the presence of a dynamic Jahn-Teller effect. However, besides the contributions to the splittings from spin-orbit coupling within the $^4T_1$ state, there are also second-order contributions from coupling with the higher $^4E(t^3e^2)$ states which are of order 10 cm^{-1}. This complicates the analysis of the $^4T_1$ exciton spectrum. Whatever may be the case, it is evident that there may be sizable mixings between the states with $m_s=-\frac{3}{2}$ and those with $m_s\neq-\frac{3}{2}$; therefore, it is important not to neglect spin-orbit interactions in discussing the two-exciton states and their selection rules.

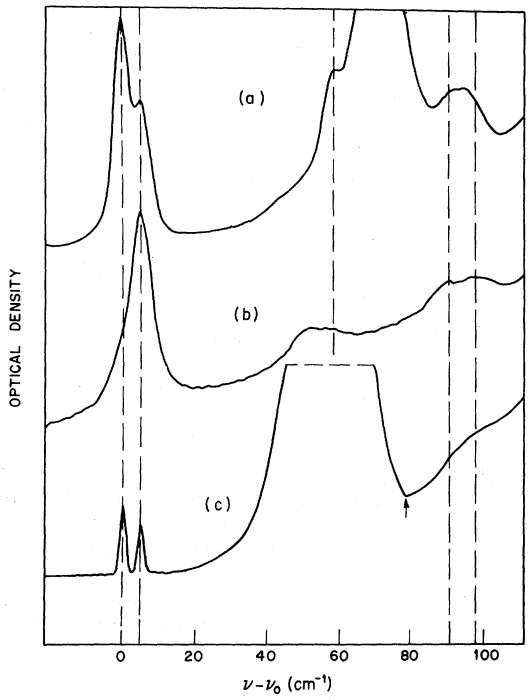

FIG. 5. Comparison of the fine structure in the absorption spectrum of $RbMnF_3$ for the (a) $^4T_1(G)+{}^4A_1$, ^4E, (b) $^4T_1(G)+{}^4T_1(G)$, and (c) $^4T_1$ transitions. The values of $\bar{\nu}_0$ are (a) 43 302, (b) 36 827, and (c) 18 227 cm^{-1}.

The $^4T_1$ exciton spectrum that we obtained is shown in Fig. 5(c). A magnon sideband peaks 57 cm^{-1} away from the lowest-energy exciton and has a sharp cutoff of intensity at 73 ± 0.5 cm^{-1} away from each exciton. The critical points which can contribute to the intensity of the magnon sideband are the L and W points. From neutron scattering experiments,[15] a measured value for the zone boundary magnon energy at the L and W points is 71 ± 6 cm^{-1}. Except for exciton dispersion effects, the energy of the magnon sideband cutoff is identical to the L-point magnon energy. (Exciton-magnon interaction effects change the shape of the magnon sideband, but not the cutoff energy.[32]) The $^4T_1$ excitons probably have less than a 0.5-cm^{-1} dispersion in $RbMnF_3$ (as they do in MnF_2). Therefore, we have a relatively accurate measure of the L-point magnon energy.

We observe only two cutoffs of the magnon sideband, corresponding to the two visible exciton lines. There is no magnon sideband seen for the apparent third transition at 18 239 cm^{-1}. Its absence is somewhat surprising since there is no se-

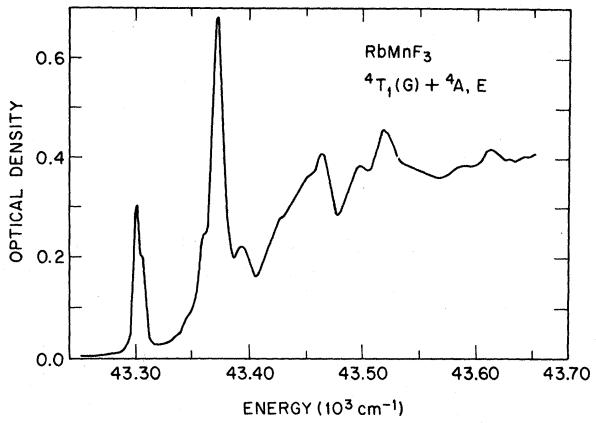

FIG. 6. Transmission spectrum in the $^4T_1(G)+{}^4A_1$, ^4E two-exciton region for a 0.1-mm-thick $RbMnF_3$ crystal. The ordinate zero is arbitrary.

lection rule forbidding it.

There are other features of interest shown in Fig. 5(c). These are three weak lines at 90, 95, and 99 cm^{-1} away from 18 229 cm^{-1}. (Although only two lines are apparent in the figure, careful analysis of the spectrum shows three lines.) A peak appears at 18 377 cm^{-1}, approximately 60 cm^{-1} higher, which apparently is the magnon sideband for these lines. These transitions could be due to the creation of single excitons or of excitons plus a phonon; unfortunately, presently there is no way to distinguish between these possibilities.

Only one $^4A_1$, ^4E exciton is seen at 25 145 cm^{-1} in the unperturbed crystal. Chen[33] observed the behavior of the $^4A_1$, ^4E excitons in magnetic fields and under uniaxial stress. Novikov *et al.*[34] investigated the effects of magnetic fields up to 300 kOe on this transition. For either uniaxial stress or a magnetic field the 25 145 – cm^{-1} line splits into two components which are believed to be the $^4E\theta$ and $^4E\epsilon$ excitons. The position of the $^4A_1$ exciton is not known at this time.

1. $^4T_1(G)+{}^4A_1, {}^4E(G)$

The spectrum in the region of the expected $^4T_1(G)+{}^4A_1, {}^4E(G)$ transitions is shown in Figs. 5(a) and 6. There are two obvious zero-phonon lines at 43 302 and 43 307 cm^{-1}. The 43 360-cm^{-1} shoulder has the same width (as determined from the derivative of the absorption curve) as the lower lines and thus is likely a third zero-phonon transition. The same applies for the barely resolved lines at 43 393 and 43 398 cm^{-1}. The sideband at 70 cm^{-1} away from the origin suggests itself as a magnon sideband. However, in the phonon band there appear strong harmonics of 70 cm^{-1} out to the twelfth harmonic. Thus, the 70-cm^{-1} peak is probably a vibronic, rather than a magnon, mode since multimagnon processes are expected to be weak.

The lowest two-exciton line occurs 72 cm^{-1} below the sum of the energies of the ^4E excitons (25 145 cm^{-1}) and the lowest $^4T_1$ exciton (18 229 cm^{-1}). This interaction energy is larger than one might expect from the changes in the excited-state exchange alone and perhaps indicates a phonon contribution even though the ^4E excitons are not strongly coupled to the lattice. We shall discuss the assignments of these lines along with those of the $^4T_1+{}^4T_1$ lines in Sec. V.

2. $^4T_1(G)+{}^4T_1(G)$

Figure 7 shows the absorption lines of the double $^4T_1$-exciton transitions with the energies listed in Table II. Twice the energy of the lowest observed $^4T_1$ exciton is about 36 460 cm^{-1}; the lowest observed two-exciton line is 370 cm^{-1} higher. In contrast, the peak of the two-exciton phonon sideband is close to twice the one-exciton band energy. This is a substantial exciton-exciton interaction. However, the large exciton-exciton interaction is not so surprising once one realizes that a fairly large lattice distortion accompanies the $^4T_1$ excitons, as indicated by a Huang-Rhys factor of about 4.5. The two Mn ions share a common fluorine anion; therefore, the presence of two excitons with their distortions on neighboring Mn ions is expected to lead to a large interaction.

There are seven lines which are visible in this region, and their energies are given in Table V. The lines 47 and 51 cm^{-1} away from the main line are not quite resolved, and there is also a weak line 5 cm^{-1} to lower energy from the main lines, which was found from an analysis of the line shape of the strong line. The 152-cm^{-1} peak has a larger width than the other lines and may be a sideband of the 36 832-cm^{-1} line.

If we compare this set of two-exciton lines with those of the $^4A_1, {}^4E+{}^4T_1(G)$ group, and also with those of the $^4T_1$ single excitons, we see that the

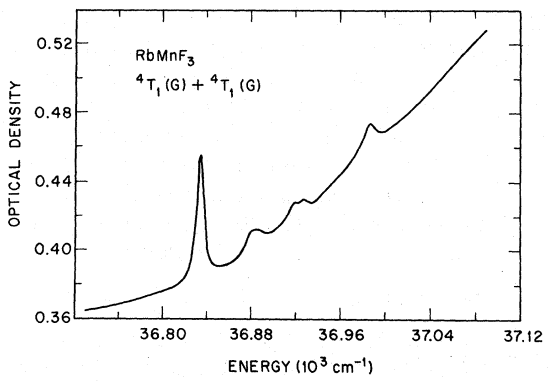

FIG. 7. Transmission spectrum in the $^4T_1(G)+{}^4T_1(G)$ two-exciton region for a 1-mm-thick $RbMnF_3$ sample.

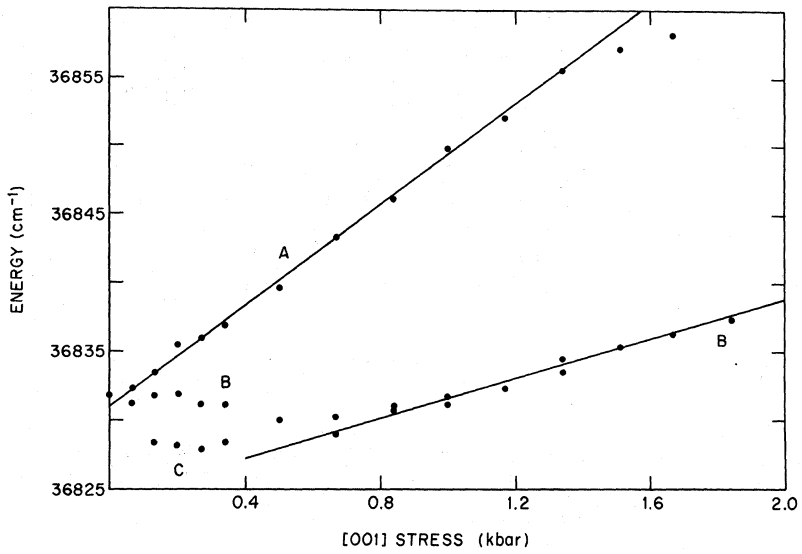

FIG. 8. Stress behavior of the lowest-energy ${}^4T_1+{}^4T_1$ exciton line in $RbMnF_3$.

groups are amazingly similar. This is demonstrated in Fig. 5. The double ${}^4T_1$ excitons appear at -5, 0, 47, 51, 85, and 92 cm^{-1} with respect to 36 832 cm^{-1}; the ${}^4A_1$, ${}^4E+{}^4T_1(G)$ excitons are at -5, 0, 53, 86, and 91 cm^{-1} with respect to 43 307 cm^{-1}; and the ${}^4T_1$ single exciton lines, at -5, 0, 85, 90, and 94 cm^{-1} from 18 234 cm^{-1}. It is hard to imagine that this is coincidental, especially the persistance of the 5–6-cm^{-1} splitting in the lowest lines. One expects that the exciton-exciton interaction would modify any splittings of the ${}^4T_1$ manifold. Since the modification is not seen, one concludes that the 5-cm^{-1} splitting is not sensitive to the exciton-exciton interaction. This is surprising since the splitting is believed to be due to spin-orbit coupling modified by a Jahn-Teller effect, which should be affected strongly by the presence of an axial field along a ⟨001⟩ axis, such as would be produced by a neighboring Mn ion in an excited state, since the exchange field and the spins lie along the ⟨111⟩ axis.

This leads us to an interesting question: Is the dispersion of the excitons sufficient such that during the lifetime of the two-exciton state the excitation can be considered as being shared by the six equivalent pairs around a given lattice site? Clearly if the double excitation resides on a given pair, the exciton-exciton interaction has axial symmetry; whereas, if the excitons are not localized, the interaction is averaged to cubic symmetry. Our results would seem to indicate the latter.

3. *Stress Behavior of* ${}^4T_1+{}^4T_1$ *Excitons*

There are twelve excitons which can be constructed from the ${}^4T_1$ manifold of Mn^{2+}. The two-exciton transitions will be observable to those combinations of states which have $m_s=-\frac{3}{2}$ character on one sublattice and $m_s=\frac{3}{2}$ on the other. In the absence of spin-orbit mixing, there are three of these on each sublattice, which can be labeled $(0,\pm\frac{3}{2})$ and $(\pm1,\pm\frac{3}{2})$. Thus, in the absence of spin-orbit coupling at most three two-exciton transitions could be seen. However, spin-orbit coupling can mix these states into higher-energy states, thereby providing transition strength for more two-exciton transitions.

Taking a cue from the success of uniaxial stress measurements in the identification of the two-exciton transitions in MnF_2, we have looked at the uniaxial stress behavior of the double ${}^4T_1$ excitons in $RbMnF_3$ in hopes of identifying the particular combinations of excitons in the ${}^4T_1+{}^4T_1$ spectrum. In Fig. 8 we show the behavior of the 36 832-cm^{-1} line under [001] stress. The component labeled A in the figure appears in σ polarization only and has an intensity of 6.5 in arbitrary units. At low stress the C line increases in intensity at the expense of the B line. However, at about 0.9 kbars the B and C lines coalesce into one line which has a polarization ratio of 4.5:1 ($\pi:\sigma$). The other two-exciton lines (not shown) split into two groups which have stress behaviors indentical to those of the A and B transitions, respectively. There are also some intensity changes such that the A group consists of the A transition plus the lines 63, 92, and 152 cm^{-1} above A, and the B group consists of the B line and lines 52, 92, and 153 cm^{-1} higher. The lines in each group have the same polarizations as the main line except for the 63-cm^{-1} line in group A which is π polarized. Under a [111] uniaxial stress no splitting or polarization of the two-exciton lines is seen, and the lines shift to higher energy at 8.5 cm^{-1}/kbar.

The stress behavior of the double ${}^4T_1$ transitions

appears not to be related to the behavior of the $^4T_1$ excitons in any simple way. Chen *et al.* observe that of the lowest three excitons, two move down in energy by 18.4 cm^{-1}/kbar and one goes up by 9.6 cm^{-1}/kbar under [001] uniaxial stress. A [111] uniaxial stress shifts all the lines down by 9.3 cm^{-1}/kbar. The two-exciton transitions show the opposite behavior! However, this behavior is not surprising once we consider the fact that the exciton-exciton interaction is quite large for the $^4T_1$ excitons. Thus, we have to consider the stress dependence of both the single-exciton energies and the exciton-exciton interaction.

In the one-exciton spectrum a [001] stress separates out the z and x, z components of the $^4T_1$ states; this splitting is measured as 28 cm^{-1}/kbar. Our measured splitting rate of the two-exciton lines above 0.9 kbars is 11 cm^{-1}/kbar. Quantitatively the stress splitting does not appear to come from this source, and one must look to possible changes in the exciton-exciton interaction energy.

The stress dependence of the exciton-exciton interaction will arise from a change in the bond length between the ion pairs. The bond length of the pair parallel to the [001] stress direction decreases by $|s_{11}P_{[001]}|$, and the bond length perpendicular to the stress increases by $|s_{12}P_{[001]}|$. Under a [111] uniaxial stress both bond lengths decrease by $|\frac{1}{3}(s_{11}+2s_{12})P_{[111]}|$. If we assign the A line to the pairs parallel to the stress and the B line to the perpendicular pairs, the polarizations of the A and B lines agree with the selection rules given in Table V, except that the B line has a small amount of intensity in σ polarization. Aside from accidental degeneracies, it is difficult to see how the B line can have intensity in both polarizations, given what we think are the symmetries of the pair. The symmetry of the pair is probably lower than we expect, perhaps because of a spin canting in the excited state. Spin canting for the perpendicular pair is a distinct possibility, since the axial field of the pair is perpendicular to the spin direction. In the excited state the anisotropy field, through the action of spin-orbit coupling, may lie along the pair axis. If the anisotropy energy is on the order of 40–50 cm^{-1}, this would lead to a detectable amount of spin canting.

In contrast to the observed stress dependence of the interaction between two $^4T_1$ excitons in $RbMnF_3$, no such effect was observed in MnF_2. This difference is probably attributable to the structure of the pairs. The primary effect of a [110] stress on the Mn-F-Mn bond in MnF_3 is a change in the bond angle; whereas, in $RbMnF_3$ a [001] stress affects the total bond length directly.

In conclusion, the explanation for the stress behavior of the $^4T_1+{}^4T_1$ exciton lines seems to be qualitatively correct, but there are many details yet to be explained.

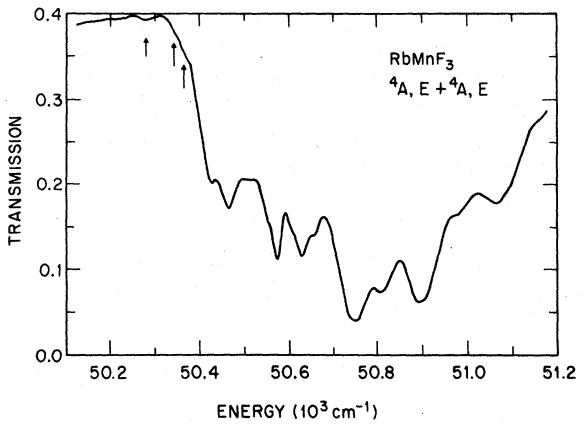

FIG. 9. Transmission spectrum in the $^4A_1$, $^4E+{}^4A_1$, ^4E two-exciton region for a 0.1-mm-thick $RbMnF_3$ crystal.

4. $^4A_1,{}^4E(G)+{}^4A_1,{}^4E(G)$

The two-exciton spectrum for these transitions is shown in Fig. 9. We observe three weak lines, which are indicated by arrows in the figure. The lowest line has an energy of 50 281 ± 4 cm^{-1} and a width of about 20 cm^{-1}, which is limited by our instrumental resolution. The absorption transition at 50 281 cm^{-1} is 9 ± 4 cm^{-1} away from twice the energy of the one-exciton state (50 290 cm^{-1}). Its energy can be affected by exciton dispersion and the exciton-exciton interaction. The proximity of this line to the expected energy of the ^4E double exciton means that, unless the two effects cancel each other, both the dispersion and the interaction between the excitons are relatively small.

The two other structures indicated in the figure may be sidebands to the 50 281-cm^{-1} line, but the possibility that they are zero-phonon lines cannot be discarded. There is also a relatively large amount of intensity in the phonon band, much larger than one might expect on the basis of the one-exciton band. The total integrated intensity in the two-exciton band is 1.2×10^{-5}, compared with 9.5×10^{-7} for the $^4A_1,{}^4E$ exciton-magnon transition.

V. SUMMARY

In this paper we have presented work on the two-exciton transitions which appear in the near-ultraviolet spectra of MnF_2 and $RbMnF_3$. From an analysis of the data we have been able to determine the source of the interaction between excitons, to identify particular two-exciton zero-phonon lines, and to discuss other properties of the two-exciton state. Although much further research remains to be done on the statics of the two-exciton combinations, a study of their dynamics has great appeal.

Of particular interest would be the possibility of producing emission from the two-exciton state or excitonic molecule by creating large numbers of single excitons with laser light. Further, the dispersion of the excitonic molecule and its possible decay modes are of interest.

ACKNOWLEDGMENTS

We wish to acknowledge R. E. Dietz and M. D. Sturge for helpful discussions; also, M. Y. Chen, D. S. McClure, and E. I. Solomon for providing us with a report of their paper. We thank A. J. Williams for technical assistance.

[1]Y. G. Litninenko, V. V. Eremenko, and T. I. Garber, Phys. Status Solidi 30, 49 (1968), and references therein.

[2]K. Betzler and T. Weller, Phys. Rev. Letters 26, 640 (1971).

[3]F. Varsanyi and G. H. Dieke, Phys. Rev. Letters 7, 442 (1961).

[4]A. L. Schawlow, D. L. Wood, and A. M. Clogston, Phys. Rev. Letters 3, 271 (1959).

[5]J. P. van der Ziel, Phys. Rev. Letters 26, 766 (1971).

[6]R. L. Greene, D. D. Sell, W. M. Yen, A. L. Schawlow, and R. M. White, Phys. Rev. Letters 15, 656 (1965).

[7]D. D. Sell, R. L. Greene, and R. M. White, Phys. Rev. 158, 489 (1967).

[8]S. J. Allen, Jr., R. Loudon, and P. L. Richards, Phys. Rev. Letters 16, 463 (1966).

[9]J. Ferguson, Australian J. Chem. 21, 307 (1968).

[10]S. E. Stokowski and D. D. Sell, Phys. Rev. B 3, 208 (1971).

[11]C. Trapp and J. W. Stout, Phys. Rev. Letters 10, 157 (1963).

[12]F. M. Johnson and A. H. Nethercot, Jr., Phys. Rev. 114, 705 (1959).

[13]A. Okazaki, K. C. Turberfield, and R. W. H. Stevenson, Phys. Letters 8, 9 (1964).

[14]P. H. Cole and W. J. Ince, Phys. Rev. 150, 377 (1966).

[15]C. G. Windsor and R. W. H. Stevenson, Proc. Phys. Soc. (London) 87, 501 (1966).

[16]R. Loudon, Advan. Phys. 17, 243 (1968).

[17]Y. Tanabe, J. Moriya, and S. Sugano, Phys. Rev. Letters 15, 1023 (1965).

[18]K. Gondaira and Y. Tanabe, J. Phys. Soc. Japan 21, 1527 (1966).

[19]R. S. Meltzer, M. Lowe, and D. S. McClure, Phys. Rev. 180, 561 (1969).

[20]W. J. Ince and A. Platzker, Phys. Rev. 175, 650 (1968).

[21]D. E. Eastman, Phys. Rev. 156, 645 (1967).

[22]D. D. Sell, Appl. Opt. 9, 1926 (1970).

[23]D. D. Sell and E. O. Kane, Phys. Rev. 185, 1103 (1969).

[24]A. Mehra and P. Venkateswarlu, J. Chem. Phys. 47, 2334 (1967).

[25]V. V. Druzhinin, R. V. Pisarev, and G. A. Karamysheva, Fiz. Tverd. Tela 12, 2239 (1970)[Sov. Phys. Solid State 12, 1789 (1971)].

[26]R. S. Meltzer and L. L. Lohr, J. Chem. Phys. 49, 541 (1968).

[27]R. E. Dietz, A. Misetich, and H. J. Guggenheim, Phys. Rev. Letters 16, 841 (1966).

[28]N. Fuchikami, J. Phys. Soc. Japan 28, 871 (1970).

[29]R. E. Dietz and A. Misetich, in *Proceedings of the Conference on Localized Excitations in Solids, Irvine, California*, 1967 (Plenum, New York, 1968), p. 366.

[30]Ming-Yi Chen, D. S. McClure, and E. I. Solomon (unpublished).

[31]It has been observed that the energies of the lowest $^4T_1$ excitons vary somewhat from crystal to crystal. This energy difference can be up to 30 cm^{-1}. It is suspected that the differences could be due to strain in the material, although the strain has to be relatively homogeneous since the linewidth only varies from 0.9 to 3 cm^{-1}. The lines with the highest energies were found to be the sharpest.

[32]R. J. Elliot, M. F. Thorpe, G. F. Imbusch, R. Loudon, and J. B. Parkinson, Phys. Rev. Letters 21, 147 (1968).

[33]Ming-Yi Chen, Ph.D. thesis (University of Chicago, 1970) (unpublished).

[34]V. P. Novikov, V. V. Eremenko, V. M. Gredeskul, and S. A. Gredeskul, Tr. Fiz. Tekh. Inst. Nizkikh. Temp. Akad. Nauk Ukr. SSR, Fiz. Kondens. Sost. No. 7, 155 (1970).